This is a previous version of the article published in Topics in Current Chemistry. 2019, 377:5. doi:10.1007/s41061-018-0228-x

Determination of Specific Electrocatalytic Sites in the Oxidation of Small Molecules on Crystalline Metal Surfaces

Manuel J. S. Farias[†] and Juan M. Feliu*[,‡]

[†]*Departamento de Química, Universidade Federal do Maranhão, Avenida dos Portugueses, 1966, CEP 65080-805, São Luís – Maranhão, Brazil*

[‡]*Instituto de Electroquímica, Universidad de Alicante Ap. 99, E-03080, Alicante, Spain*

*Corresponding Author: juan.feliu@ua.es (J. M. Feliu); phone: +34 965 909 301

ORCID of the authors:
M.J.S.F.: 0000-0001-8531-3388
J.M.F.: 0000-0003-4751-3279

Abstract

The identification of the active sites in electrocatalytic reactions is part of the elucidation about of mechanism of the catalyzed reactions on solid surfaces. However, this is not an easy task, even for apparently simple reactions, as we sometimes think is the oxidation of adsorbed CO. For the surfaces consisting of non-equivalent sites, the recognition of specific active sites must consider the influence that facets, as is the steps/defect on the surface of the catalyst, cause in its neighbors; one has to consider the electrochemical environment under which the "active sites" lies on the surface, meaning that defects/steps on the surface do not do chemistry by themselves. In this paper, we outline the recent efforts in understanding the close relationships between site-specific and the overall rate and/or selectivity of electrocatalytic reactions. We approach the hydrogen adsorption/desorption, and oxidation CO electro-oxidation, methanol, and ammonia. The classical topic of asymmetric electrocatalysis on kinked surfaces is also addressed for glucose electro-oxidation. The article takes into account selected existing data combined with our original works.

Keywords: Electrocatalysis, single crystal surfaces, active sites, structure sensitivity, asymmetric electrocatalysis.

1. Introduction

Generally, the catalysts consist of non-consumable chemicals capable of providing a favorable energy landscape for mediating steps chemical reactions. The catalysts can be found everywhere in nature, as is the case of the enzymes in living world, which are extremely selective [1]. In the case of inorganic catalysts, the efficiency almost always needs to be improved [2]. In heterogeneous catalysis, the catalyst materials very often are solids – such as the oxides or metals on a support – and the reactants are found in fluid phase – as is the gaseous phase or liquid one. The mechanism through which the reactions proceed on a catalyst surface is complex, involving many reaction intermediates, and it is worth to say that many parameters, which can be intrinsic and extrinsic to the catalyst surface, influence its overall efficiency [3]. The efficiency of the catalysts can be (and had historically been [2]) improved by trial-and-error, but this strategy is very time consuming and does not allow to push the limits of the efficiency of the catalyst in terms of both activity and selectivity (and also long-term stability). The factors underlying the efficiency in heterogeneous electrocatalysis only can be reached if in-depth knowledge about the molecular relationships between the catalyst surface structure and the reactants/reactions taking place on it is successfully achieved. In this regard, from the theoretical viewpoint, it has been proposed that energy scaling relations, *i.e.*, for catalyzed reactions on the surface of some transition metals, the binding energies of adsorbed intermediates correlate with each other and this scaling relations likely limit the catalysis efficiency [3, 4]. This theoretical perception on catalysis has been extremely influential in the interpretation of heterogeneous catalysis at the solid/gas interface [5].

In electrocatalysis, the catalysts are immersed in an electrolyte with which interact, so that the catalyst surfaces are never unoccupied or "clean" as in ultra-high vacuum (where it is required pressure below ~10^{-9} torr so that the surface be kept "clean" for up to about 1 hour [6]). In this sense, beyond a parameter as the external applied potential, also absent in the ordinary heterogeneous catalysis, in electrocatalysis the catalyst surface permanently interacts also with generally water-based electrolyte and its ions (and, not to say, the surface impurities coming from the electrolyte). This means that, during the attachment of the reactants to the catalyst surface, competitive reactions always take place. However, as in the heterogeneous catalysis, in electrocatalysis the rate of reaction and the selectivity may be tactically tuned, playing with characteristics intrinsic to the electrode/catalyst surface, as the structure of the surfaces, as the shape of nanocrystals and step site density [7-9]. In addition, the catalytic activity can be modified based on parameters extrinsic to the catalyst surface, as is the electrolyte composition, the effect/influence of anions and, more recently pointed out, cations (still not well understood), pH of the solution [10, 11].

In controlled experiments, the structure sensitivity character is successfully accessed by controlling the specific atomic configuration on the catalyst surfaces [12]. Notwithstanding, despite that surface-structure-sensitivity relationships are easily pointed out, the determination of the exact structure of the *active sites* involved in a specific reaction pathway is not trivial and requires a great number of high quality experiments in fundamental electrocatalysis. For electrocatalyzed reactions, this subject has been addressed in two review articles few years ago [9, 13]. With regard to the surface structure, it is well established that the studies at the single crystal surfaces has historically played a prominent role in advances for understanding on molecular factors in heterogeneous catalysis at both solid/gas [6] and solid/liquid electrified interface [14]. The suitability of the studies with single crystal surfaces – as a step in the direction

for understanding about the structure-activity relationships – is because the single crystal surfaces simplify enormously the number of variables of the catalytic process, and the single crystal, at certain level, mimics the facets of the catalysts nanoparticles used in the real applications.

The identification of active sites requires the design of specific experiments for the description and investigation of the causes of the reactivity, catalytic activity and selectivity in heterogeneous electrocatalysis [15, 16]. In this article, we discuss efforts devoted to the establishment of relationships between reactivity and surface reaction pathways for the following electrochemical reactions: hydrogen adsorption/desorption reaction, electro-oxidation of CO, methanol, ammonia and glucose on platinum single crystal electrodes. It is worthy to notice that the significance of these reactions in the field of electrocatalysis is because they are surface structure sensitive reactions. The hydrogen adsorption/desorption and oxidation of carbon monoxide reactions can serve as surface model reactions. The oxidation of methanol and ammonia can serve as examples of potential fuel in low temperature fuel cells. Moreover, the study of ammonia oxidation has a great appeal for environmental issues. The electro-oxidation of the glucose is the best-documented case of enantiospecific interaction between a chiral molecule and an intrinsically chiral surface.

2. The Structure of the Catalytic Substrate

In heterogeneous electrocatalysis, the catalytic events, *i.e.*, all the elementary reaction steps into the catalytic cycle, take place on the topmost layer of the atoms at the catalyst. The atomic ensemble at the surface where reaction takes place, involving the reaction intermediates and transition states, combines the effect of both electronic and geometric nature and is simplified under the name of surface active sites. In this sense, the active sites are far from being atoms, but structures that eventually may have some level of synergy. Historically, from a surface structure point of view, the insight on the active sites is attributed to Taylor and backs to 1925 [17]. Taylor reviewed the question about the mechanism of the catalytic action in solid surfaces, and he concluded that the occurrence of the reactions on surfaces was restricted to occur on unsaturated surface atoms [17]. In fact, in the real world, the surfaces of the catalyst consist of non-periodical arrangement of atoms, resulting in different local chemical environments [18]. As an example, the different configurations of atoms at the catalyst surfaces can be represented by a crystal surface model, as illustrated in Figure 1 for crystals of the fcc (face centered cubic) lattices.

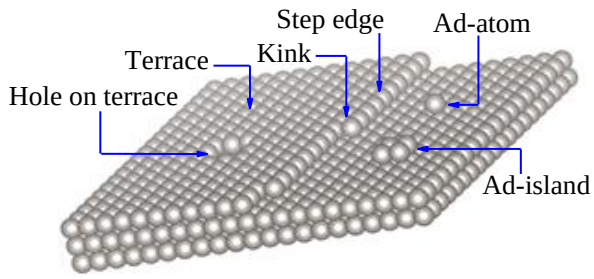

Figure 1. Hard sphere model of a Pt(111) surface, indicating different features: terrace, step, kink, hole, ad-atom and ad-island atoms.

The surface in Figure 1 contains terrace, step-edge, kink, ad-atom, ad-island and hole atoms. Under this framework, it is usually considered that the surface structure stays stable during the reaction, which could not be the case. Also, the uncontrolled crystallographic features such as holes, ad-atoms or ad-islands are not considered. In practice, the unevenly distributed sites or atom arrangement at surfaces, reflect in the variation of the local physical properties intrinsic to the surfaces as is the work function [19, 20], and imperfections, as the steps, create electronic perturbation on the terraces [21]. These modifications at the catalyst surface originate deep consequences in the catalytic properties and open the possibility of tuning the properties of the catalyst, in a controlled way. In fact, there are surface catalyzed reactions which preferentially takes place at the low coordination sites, typically at step or kink sites while there are others reactions which occurs preferentially at terraces [22].

Attempts to classify the electrocatalytic reactions as to their dependence on the surface structure (and size scale) of the electrocatalytic materials has been appeared in literature [9]. However, beyond the structure of the topmost layer of atoms at the surface, combining the effects of electronic and geometric nature [23], the electrocatalytic properties very often depend on factors external to the structure of the catalyst surface, *i.e*., the electrochemical environments where the "active sites" exists at the catalyst surfaces. On this regard, the nature of anions and cations of the electrolyte and its pH also exert influence on the performance of the catalyst. In fact, at different potentials, the nature of anions and its ability (and strength) to attach on the catalyst surface can induce the preference of reaction pathways [24]. In the case of solution pH, the mechanisms by which this parameter affects the catalytic activity are much more complex than previously thought. In this sense, at the surface of a same catalyst (consisting of non-equivalent sites), the change of solution pH passing from acidic toward alkalinity catalytically favored some kind of sites (as highly coordinated Pt atoms, the (111) terrace sites), while the catalytic activity of the sites consisting of low coordination atoms was inhibited [25]. Then, the recognition of the active sites in electrocatalysis involve at least two environment aspects: one intrinsic to the catalyst surface, involving geometric and electronic factors (which include scale or size factors) and the possible influence of the local electrochemical environment (extrinsic to the catalyst surface). Both aspects determine the catalytic properties of the active site in electrocatalysis. In the following, some of these aspects, such as surface structure, would be considered constant unless otherwise stated, under the whole experiment, but others would vary with applied potential.

3. Determination of Specific Electrocatalytic Sites

3.1. Fingerprints of Step and Terrace Sites on Pt Surfaces as Probed by Hydrogen Adsorption/Desorption

In Pt surface electrochemistry, the so-called hydrogen region is recognized to be a fast, surface limited, faradaic charge transfer reaction as a result of proton discharging to adsorbed hydrogen and its reverse reaction: $H^+ + e^- + *_{active\ sites} \rightleftarrows H_{ads}$. These reactions correspond to the under potential deposition of hydrogen (H_{UPD}), and is a characteristic signature of few transitions metals in periodic table, such as Pt, Rh, Pd and Ir. At platinum electrodes in contact with different test electrolytes, as $HClO_4$, H_2SO_4, NaOH, those reactions develop well-defined reversible voltammetric features at potentials several mV higher than hydrogen evolution which serve as a fingerprint of Pt crystal facets and can be used to identify Pt active sites [26, 27]. In a spectro-electrochemistry study, in the region of H_{UPD} at 0.1 V_{RHE}, a band at 2080-2095

cm^{-1}, attributed to H_{ads} on top sites, was characterized by surface-enhanced infrared absorption spectroscopy [28]. A single band, assigned to the Pt-H_{ads}, also has been observed for Pt at the solid/gas interface [29]. However, other geometries of adsorbed hydrogen at potentials of H_{UPD} on Pt, as is the hollow sites, have been considered [28]. Then, because at the potentials range of H_{UPD} the surface is predominantly covered with H_{ads}, it is plausible to assume that the proton discharging onto adsorbed hydrogen involve at least the reaction of water displacement from the Pt surface at potentials of H_{UPD}: Pt-[$(H_2O)_m$] + H^+ + e^- ⇄ Pt-H_{ads} + mH_2O. As the potential increases in the positive direction, the characteristics of the electrified interface favors the Pt surface interaction with anions. Recently [30], attempts to provide a most complete description of the possible interfacial events responsible for the features in the "hydrogen" region include the possible participation of cations interacting with the Pt surface, and attempts to explain the non-Nernstian pH dependence of the "hydrogen" peak in voltammogram.

The voltammetric behavior of Pt single crystals in contact with a 0.1 M $HClO_4$ solution are displayed in Figure 2, for three single crystal surfaces. The two stepped surfaces, namely Pt(554) and Pt(544), consist in 9-atom wide (111) terraces, which are periodically broken by monoatomic steps with (110) and (100) orientation, respectively. The visible peaks caused by hydrogen adsorption/desorption at the (110) and (100) steps are distinctly separated by ~156 mV. Figure 2 also shows a hard sphere model for each surface orientation, indicating the position of the monoatomic steps and 2-dimensional (111) domains on the surfaces. The qualitative difference in the voltammetric profiles in the potential range of ~0.06 up to ~0.35 V_{RHE} concerns in the existence of the remarkable peaks at ~0.128 and ~0.284 V_{RHE} due to the hydrogen adsorption/desorption at the (110) and (100) monoatomic steps, respectively. As we can see in inset of the Figure 2 for the hard sphere model, the row of monoatomic steps consists in two parts: the top side and the bottom one, that would correspond to the positive and negative sides of the dipole steps, following the Smoluchowski model [31]. The reversible peaks in the corresponding voltammetries, therefore, are the fingerprint of the (110) and (100) step sites at Pt surfaces containing relatively wide (111) terraces. These peaks are completely absent in the cyclic voltammogram of Pt(111) surface, which should contain only the (111) terraces. Details on the voltammetric profile for range of potentials upper to hydrogen region specially for the Pt(111) surface in perchloric acid are available elsewhere [32-34].

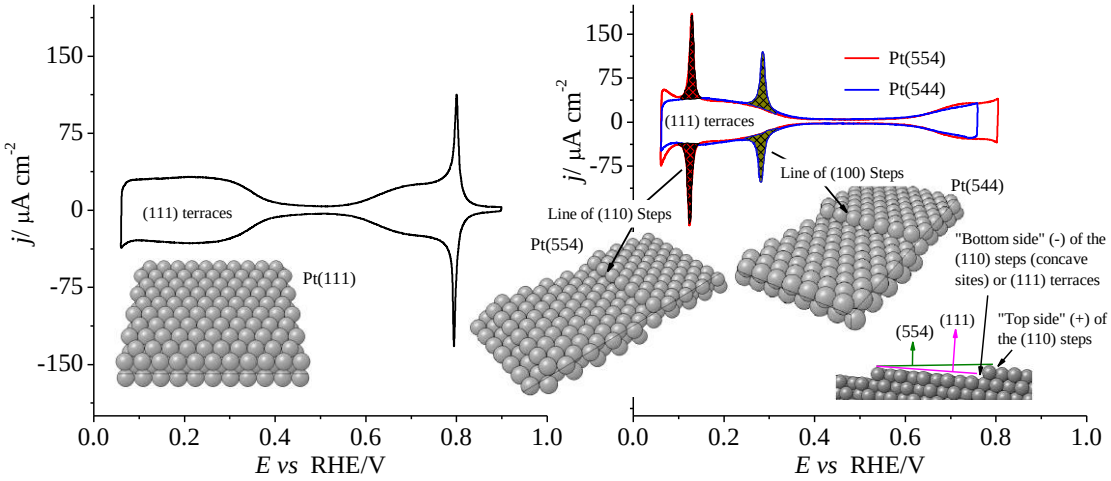

Figure 2. Cyclic voltammograms of Pt crystal surfaces, namely, Pt(111), Pt(554) and Pt(544), in 0.1 M $HClO_4$ recorded at potential sweep speed of 50 mV s^{-1}. Data include illustrations of hard sphere models for each surface orientation.

On the basis of H_{UPD} redox reactions taking place at site-specific Pt electrodes, it is possible to use the electric charge under the different states to estimate the coverage of blocking species which binds at the Pt sites stronger then H_{ads} does, and consequently displace H_{ads} from the surface. If the blocking species is site-selective, then monitoring the changes of the voltammetric profile in the hydrogen region, it would be possible to identify the specific electrocatalytic sites for an electrocatalytic reaction. The reverse is also possible, *i.e*., when a strongly blocking species leaves the surface and the vacancy sites become available for H_{UPD}. Therefore, it is possible to use the sequence of changes of the hydrogen region with the aim of surface sites assignation for some electrocatalytic reaction. One of these reactions is the CO electro-oxidation.

3.2. Electro-oxidation of Carbon Monoxide

Similar to the solid/gas interface [35, 36], the adsorption and oxidation reaction of CO can be considered a model in surface electrochemistry and electrocatalysis [37, 38]. From the fundamental research viewpoint, the CO oxidation reaction is widely used as a first test in heterogeneous catalysis and has been widely used as a model for the development of concepts in this field [35]. In surface electrochemistry, the adsorption of CO is employed in obtaining information about the structure of the electrified interface, as is the determination of the potential of zero total charge [39] for different electrodes. The charge that crosses the electrode/electrolyte interface during the electro-oxidation of a CO monolayer can serve as a parameter for quantitative estimation of "electrochemically active surface area" (EASA) of the catalyst surfaces. Thus, the determination of EASA by CO stripping procedure has been revealed to be more accurate than the use of the charge from the H_{UPD} [40, 41], likely because the latter is more sensitive to surface contamination. It should be noted, however, that agreement is found if controlled experiments are performed [39]. On the other hand, adsorbed CO appears as intermediate in the electro-oxidation of carbon containing compounds (such as alcohols and other organic species[42]), and from the kinetics point of view, the self-generated CO_{ads} species act as a catalytic poison.

Studies on the electro-oxidation of CO adlayer by voltammetry employing stepped Pt surfaces, as a general rule, revealed that in acid media the voltammetric stripping presents a single oxidation peak (not considering the possible pre-oxidation process), and the potential of CO oxidation peak shifts to lower values as the density of steps increase on the Pt surface [43], Figure 3. In these specific experiments, the electrode preconditioning consisted of flame annealing and cooling under a controlled Ar/H_2 atmosphere. Additionally, the CO adlayer was deposited with the potential fixed at 0.100 V_{RHE}. The significance of highlighting this is because there are exceptions to that general rule [44], in which the catalytic activity of the platinum is greatly influenced by the catalyst preconditioning and the adsorption conditions of the CO adlayer. In alkaline media, on the other hand, the voltammetric CO stripping from Pt stepped surfaces exhibits more than one CO oxidation peaks, as shown in Figure 4. At Pt(111) the main peak is observed at 0.78 V, while the electrodes with (110) steps show another peak at 0.6 V and those with (100) steps at 0.7 V. At first glance, the catalytic behavior in alkaline media *is not* related to the greater "availability" of OH_{ads}, as is often suggested for experiments in alkaline media. The important issue that arises deals with

the types of active sites that correspond to the different peaks of CO oxidation in the voltammograms, and the role that water plays in that reaction.

In the reaction of CO electro-oxidation, different from the studies at the solid/gas interface, in which the oxygenated species is coming from molecular oxygen, at the aqueous electrified solid/liquid interfaces, it is accepted that the source of oxygenated species comes from the water molecules. It is also almost consensual that the mechanism of the electrocatalytic CO oxidation proceeds through the Langmuir-Hinshelwood mechanism type, in which bi-molecular interaction between two neighboring adsorbed species, *i.e.*, CO_{ads} and (presumably) any sort of activated water, as proposed by Gilman [45], or incipient OH_{ads}, react to form the CO_2, which desorbs readily to free up the active sites on surface. The overall reaction of CO electro-oxidation (disregarding any adsorption of anions, which certainly play an important role in the process [46] can be written as:

$$Pt_{\alpha}\text{-}CO + Pt_{\gamma}\text{-}(H_2O) \rightarrow CO_2 + 2H^+ + 2e^- + (\alpha + \gamma)Pt \qquad (1)$$

in which the term α and γ stands the number of Pt atoms involved in the adsorption of each species. The standard potential for the reaction $CO_{(g)} + H_2O_{(l)} \rightleftarrows CO_{2(g)} + 2H^+ + 2e^-$ is $E^0 \simeq -0.104$ V_{SHE}.

In the catalytic process of the electrochemical water dissociation to OH_{ads}, protons and electrons are expelled, *i.e.*, $H_2O + *_{active\ sites} \rightarrow OH_{ads} + H^+ + e^-$. This reaction is expected to occur on Pt electrodes, at least at high potentials. In acidic media (0.1 M HF), Ueno *et al.* [47] using *in situ* infrared spectroscopy have provided evidences that the reaction of OH_{ads} formation, on stepped Pt surfaces (consisting of (111) terraces separated by monoatomic (110) or (100) steps, as in Figure 2) starts at ~0.3 V_{RHE}. The reaction of OH_{ads} formation depends on the adsorption sites and the applied potential. At least at 0.9 V_{RHE}, the OH_{ads} on (111) terraces is dominant in comparison to the OH_{ads} on step sites; OH_{ads} coverage, *i.e.*, the band intensity of δ_{PtOH} (in-plane bending mode of OH_{ads}), decreased with the increase in step density [47]. If this (independent) reaction takes place in a step of the CO electro-oxidation, a possible intermediate species formed during CO_{ads} electro-oxidation would be the $COOH_{ads}$ species, whose formation depends on the structure of the electrode, but its decomposition to CO_2 is potential dependent, *i.e.*, $COOH_{ads} \rightarrow CO_2 + H^+ + e^- + *_{active\ sites}$. Santos *et al.* [48] had already proposed that $COOH_{ads}$ might be a reaction intermediate during the electro-oxidation of CO_{ads} on Pt in acid media. However, the chemical nature of the oxygenated species that react with CO_{ads} remains an open question.

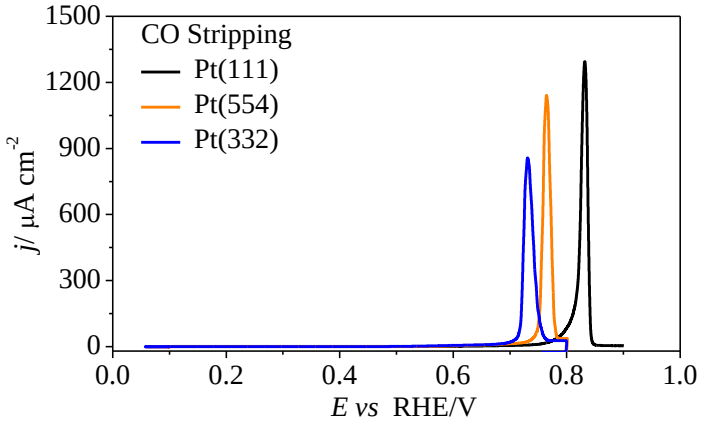

Figure 3. Electro-oxidation of CO adlayer on Pt(111), Pt(554) and Pt(332) in 0.1 $HClO_4$. The CO adlayer was deposited at 0.10 V_{RHE}. Data recorded at sweep rate 50 mV s^{-1}. The data were reproduced and adapted from [49] American Chemical Society with permission and [25] Elsevier with permission.

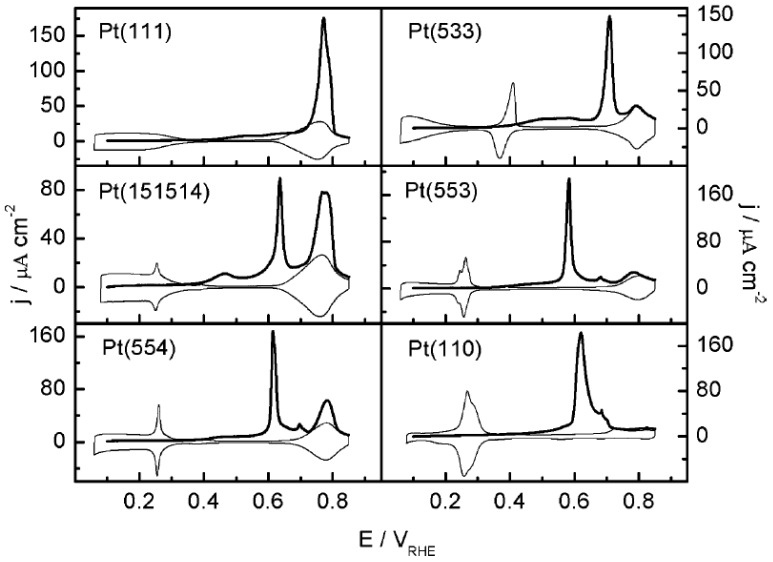

Figure 4. CO stripping (thick solid line) and the subsequent cyclic voltammogram (thin solid line) for Pt(111), Pt(151514), Pt(554), Pt(533), Pt(553) and Pt(110) in 0.1 M NaOH. The CO adlayer was deposited at 0.10 V_{RHE}. Data recorded at sweep rate 20 mV s^{-1}. The data were reproduced and adapted from [50] Royal Society of Chemistry with permission.

The identification of active sites in the CO electro-oxidation refers to experiments of CO stripping, which is when there is no CO beyond that adsorbed on the catalyst surface. The comparison between CO and H adsorption is useful because H cannot adsorb on CO-covered sites. In a full CO adlayer at Pt stepped surfaces such as those of Figure 2, it is plausible to assume that all kind of sites are occupied by CO, *i.e.*, either the (111) terrace sites and the step sites are blocked by CO. At this stage of full CO coverage (and in absence of solution CO), we can partially to remove the CO adlayer and verify the kind of sites released after CO electro-oxidation. It is appropriate to anticipate that this experimental procedure is because the CO_{ads} adlayer apparently behaves as a typical poison ("immobile") layer during the CO_{ads} is oxidation. In the last five years, we have conducted a series of experiments in this direction in the entire pH range, and it was found that at stepped Pt surfaces the most active sites consist in (111) terraces [25, 51, 52]. The intrinsic catalytic activity of step and kink sites is lower compared to the catalytic activity at the (111) terraces of those kinds of surface. In this framework, concerning to the determination of specific electrocatalytic sites in CO oxidation, other example is shown in Figure 5 for a Pt(554) surface in 0.1 M NaOH, whose CO_{ads} adlayer was formed at 0.100 V_{RHE}. In Figure 5 the (110) steps were selectively blocked by CO adsorption. In this case, in comparison to the blank cyclic voltammogram (red line), the reversible pair of peaks at ~0.264 V are fully blocked for hydrogen adsorption, and only the sites at the (111) terraces were free to adsorb hydrogen (Figure 5 – olive line). The oxidation of the CO only on (110) steps develops a peak at ~0.79 V. On the other hand, in the oxidation of full coverage CO, where presumably all the kind of sites were occupied by CO, the voltammetry develops multiple CO oxidation peaks. In the case of CO electro-oxidation on kinked Pt surfaces in alkaline media, three oxidation peaks arise in CO stripping voltammogram [53]. For full coverage (Figure 5), one prominent peak appears at ~0.58 V, and on the basis of partial CO stripping, it is due to the CO electro-oxidation along the (111) terrace sites of the Pt(554)

surface. The position of this peak is extremely sensitive to the surface orientation (and flame annealing preconditioning). Then, in the Figure 5, the potential required for the CO electro-oxidation involving the (111) terraces is lower than that required for the CO oxidation at the (110) steps or top side of the step sites. Therefore, it is clear that the electro-oxidation of CO at Pt surfaces is a reaction which preferentially takes place at (111) terrace sites. Even the kink sites are less catalytically active toward CO electro-oxidation than the (111) terrace sites of the kinked Pt surfaces [51]. The identification of the (111) terraces of the stepped Pt surfaces as being the most active sites also has been possible by *in situ* FTIR [51, 52, 54]. On the other hand, on the basis of theoretical (coordination-activity plot) modeling (and experimental data), Calle-Vallejo *et al*. [55] suggested that the Pt sites what become activated at lowest potentials are located at convex structures, being OH_{ads} at the top side of the steps, whereas the CO_{ads} were at the (111) domains from the upper side of the (111) terraces (close to the step occupied with OH_{ads}). Preferential CO electro-oxidation at the (111) terraces has also been observed on shape-controlled Pt nanoparticles (size about ~8.5 nm) in alkaline media [56], and on commercial carbon-supported Pt nanoparticles (mean size 1.81 nm) in acid [57].

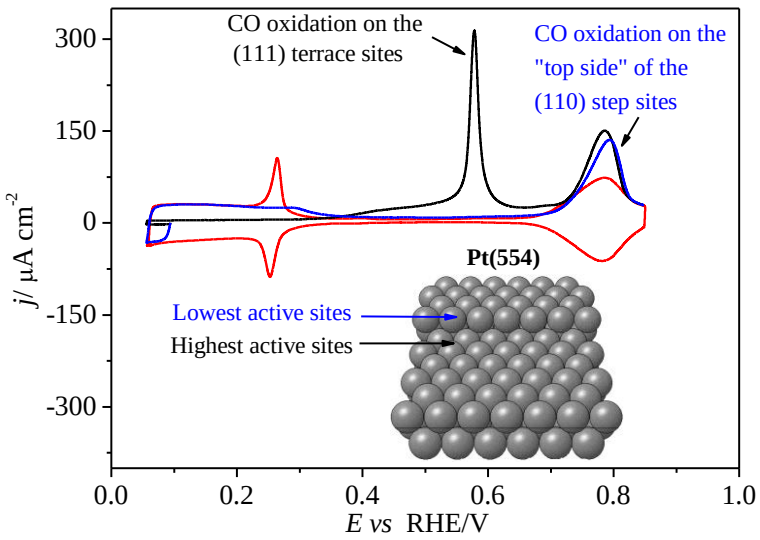

Figure 5. Determination site specific for the CO electro-oxidation at a Pt(554) surface in 0.1 NaOH. Black line: electro-oxidation of CO full coverage. Blue line: oxidation of CO only at the (110) step sites. Red line: black voltammetry. Inset: Inset: side view of the hard sphere model of the Pt(554) surface, highlighting the locally concave structure and convex one of the step site. Experiments performed at potential sweep speed of 0.05 V s^{-1}. The data were reproduced and adapted from [49] American Chemical Society with permission.

However, despite the higher catalytic activity along the (111) terraces of the stepped Pt surfaces, the catalytic activity of the Pt(111) electrode is lower than that observed for stepped surfaces in similar conditions. This can suggests that the break of the (111) terraces by steps induces variation in catalytic activity along the (111) terraces, not present in the “infinite” Pt(111) surface. In this way, on the basis of sequential sites for the CO adsorption and the oxidation at stepped Pt surfaces, it was suggested that there is a hierarchical energy gradient along the terraces [51]. In this sense, in terms of site occupancy, the top side of the step sites represents the set of sites that are preferentially occupied by CO adsorption, *i.e*., the

set of sites to be first occupied, which also are the same sites which were the last released after CO electro-oxidation, in this particular case. At solid/gas interface, in an experiment in which the CO_{ads} was forced to shift from steps to terraces and *vice versa*, as a function of a local thermal perturbation, it was observed that CO occupies preferentially the top of the steps, where it binds more strongly than on (111) terraces [58]. The set of sites close to the step sites from the bottom side (or terrace sites – see hard sphere model in Figure 5) are concave sites and are the set of sites to be the last occupied by CO adsorption, but during the oxidation of the CO adlayer, these sites are released first [51]. Then, the most catalytically active sites (locally concave structures) and the lowest catalytically active ones (locally convex structures) are present of the same local structure at the Pt surfaces [51, 52] (see inset in Figure 5). This means that the defects/steps do not do chemistry by themselves but step sites act modifying the catalytic properties of their neighboring sites. This seems to be a general characteristic of the sites vicinal to Pt(111) toward CO electro-oxidation. Recently, we have reported a case in which the activation pathway of CO oxidation on Pt was inhibited as the (111) planes become defect-rich. In this case, the CO adlayer was deposited during cooling of the Pt(111) surface in a CO atmosphere.[44] This means that the active site designation for the CO electro-oxidation requires a precise specification of the experiments.

In electrocatalysis of CO stripping experiments, after CO_{ads} oxidation at the most active sites, CO molecules do not occupy them again, because the CO_{ads} behave as an "immobile" species during the process. This is a general characteristic of CO stripping on Pt electrodes in entire pH range [25, 51, 52]. Then, based on these arguments, in terms of site occupancy, the set of the most catalytically active sites become occupied only under conditions of full CO coverage or if there is CO in the solution side. If we consider the (111) terraces and steps/defects, the strength of CO adsorption at the specific sites is a parameter which must be considered in the kinetic analysis of the preferential electrocatalytic oxidation of CO, and this preference is directly linked to the local arrangement of atoms at the catalyst surface. In this regard, the influence of (100) steps in improving catalytic activity of (111) terraces is lower in comparison to the catalytic shift in (111) terraces in presence of (110) steps, despite the intrinsic catalytic activity of the (110) and (100) steps are very similar to each other [25].

In conclusion, the most active sites toward CO electro-oxidation at the Pt(111) vicinal surfaces consists in those located on the (111) terraces. A descriptive experiment which elucidates this issue starts by decoration of the (110) steps by ^{13}CO leaving all the (111) terraces sites of a Pt(332) surface free for electro-oxidation of the CO_{ads} coming from (10^{-3}-10^{-1} M) ethanol dissociation [59]. It was shown that $^{13}CO_{ads}$ previously attached at the (110) steps oxidized at potentials higher than the electro-oxidation of CO_{ads} from ethanol dissociation at the (111) terraces of the stepped Pt surface. Again, a series of experiments including cyclic voltammetry (partial CO adlayer stripping), chronoamperomety (potential steps), and *in situ* FTIR employing well-defined Pt-based electrodes, indicate that CO_{ads} behaves as an immobile species during its oxidation [52, 60]. The oxidation of the CO adlayer initiates at sites at the bottom side of the steps, that belong to the (111) terraces. It is in this sense that we propose that the (111) domains of the stepped surfaces contain the most active sites toward CO electro-oxidation. The reaction proceeds along the (111) terraces, which became free for H_{UPD}, and the last set of sites at which the CO_{ads} was oxidized are the step sites, which were finally accessible to H_{UPD}.

3.3. Pathways of Methanol Electro-oxidation toward Carbon Dioxide

The main reason why the electrochemical oxidation reaction of methanol is so widely studied is because its potential use in low temperature fuel cells.[61] In term of thermodynamics, the standard potential for the reaction $CH_3OH_{(l)} + H_2O_{(l)} \rightleftarrows CO_{2\,(g)} + 6H^+ + 6e^-$ is $E^0 \simeq 0.016\ V_{SHE}$ and the theoretical fuel cell efficiency is $\varepsilon \simeq 96.7\%$. At platinum electrodes, it is argued that the electrochemical oxidation reaction of C_1 molecules, as methanol, formaldehyde and formic acid, can proceed through two (parallel) pathways, termed direct and indirect [62, 63]. The terminologies for these reaction pathways have the CO_{ads} as a watershed in the reaction mechanism, and the preferred pathway depends on the nature and composition of the catalyst materials, as well as on the precise local geometric arrangement of the atoms at the catalyst surfaces, as deduced from the studies on the single crystalline surfaces [64, 65]. The direct pathway is kinetically faster and it is believed that the C_1 molecules goes to CO_2 without going through CO_{ads}. The indirect one is kinetically slower, and the C_1 molecules are finally transformed in CO_2, but through CO_{ads}. In the case of formic acid (HCOOH), the direct pathway involves its dehydrogenation and subsequent evolution to CO_2. The formate species adsorbed ($HCOO_{ads}$) through the carbon atom has been identified and its possible role in kinetics – if it acts like a catalytic poison or intermediate reaction – has been warmly debated in literature [66-68]. In the indirect pathway, the C_1 molecules are dehydrated toward CO_{ads}, which displays the role of a catalytic poison, as it is oxidized to CO_2 at high potentials.

The use of Pt single crystals in studying the electrocatalysis of methanol oxidation has revealed that the reaction is strongly sensitive to the catalyst surface structure [69]. Then, on platinum, the reaction yields formic acid and formaldehyde as soluble products, while CO_{ads} is detected at the electrode surface [69]. After a kinetic study employing stepped Pt surfaces, it was concluded that methanol dissociation takes place exclusively at the step sites [65]. In these unpoised terraces, it has been shown that the direct path of methanol electro-oxidation is a site-demanding process. The quantification of this statement was experimentally determined [70] employing a cyanide-Pt(111) modified electrode, as shown in Figure 6 [70]. In the series of *in situ* FTIR spectra in Figure 6(C), no bands due to the intermolecular stretching frequencies of adsorbed CO_{ads} were detected (which should appear at ~2060-2075, and ~1850 cm^{-1}, due to the linearly and bridge bonded CO, respectively [71]). The absence of CO_{ads} in the mechanism of methanol electro-oxidation on cyanide-Pt(111) modified electrode also explains the stability of the voltammetry in the hydrogen region, even in presence of methanol in solution (Figure 6(A)). The band due to CO_2 appears in the *in situ* FTIR spectra at 2343 cm^{-1} at ~0.6 V_{RHE}, that is the onset potential for the methanol oxidation to CO_2 on cyanide-Pt(111) modified electrode.

Concerning to the surface structure of the cyanide-modified Pt(111) electrode, Figure 7(A) shows the pattern of the Pt sites occupied by cyanide. The configuration of the cyanide-modified Pt(111) electrode is a $(2\sqrt{3}\times2\sqrt{3})R30^o$ structure and provides a limited arrangement of contiguous Pt atoms [72]. The formation of CO_{ads} requires a large atomic ensemble, at least three contiguous atoms of platinum [70]. This specific atomic configuration is not observed on cyanide-modified Pt(111) electrode, explaining the direct oxidation of methanol toward CO_2, without going through CO_{ads}. The Figure 7(B-C) displays the possible matches between the configurations involving three Pt atoms on the catalyst surface and the possible reaction pathways.

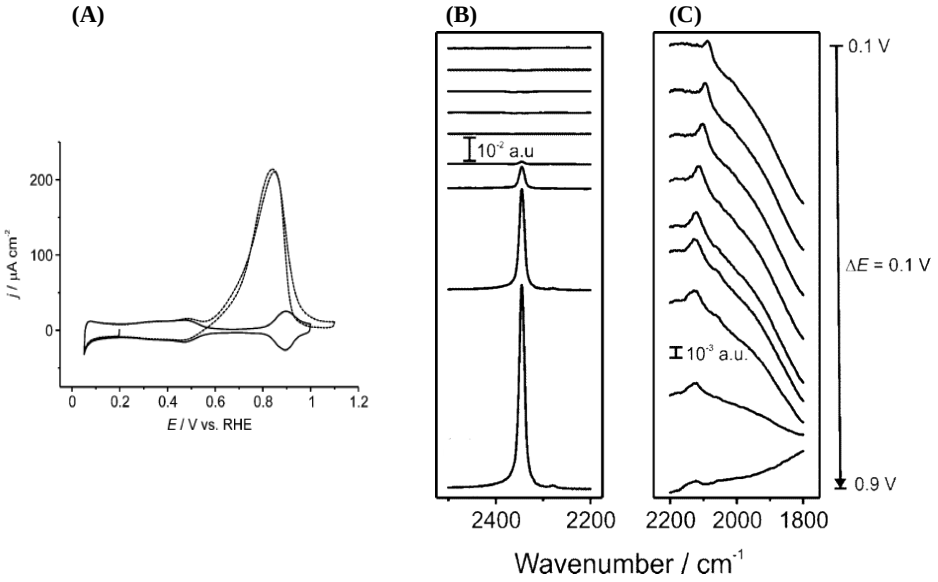

Figure 6. Electro-oxidation of 0.2 M methanol on a cyclic voltammogram of a cyanide-modified Pt(111) electrode in 0.1 M $HClO_4$. (A): cyclic voltammogrametries (methanol electro-oxidation + blank cyclic voltammograms). (B) and (C) are *in situ* FTIR spectra. The spectra in the frequency region between 2500 and 2200 cm^{-1} (B) were calculated using the spectrum at 0.05 V_{RHE} as reference, while the spectra in the frequency regions between 2200 and 1800 cm^{-1} (C) were calculated using the spectrum at 1.30 V_{RHE} as reference. The original figures were modified. Data reproduced from [70] American Chemical Society with permission.

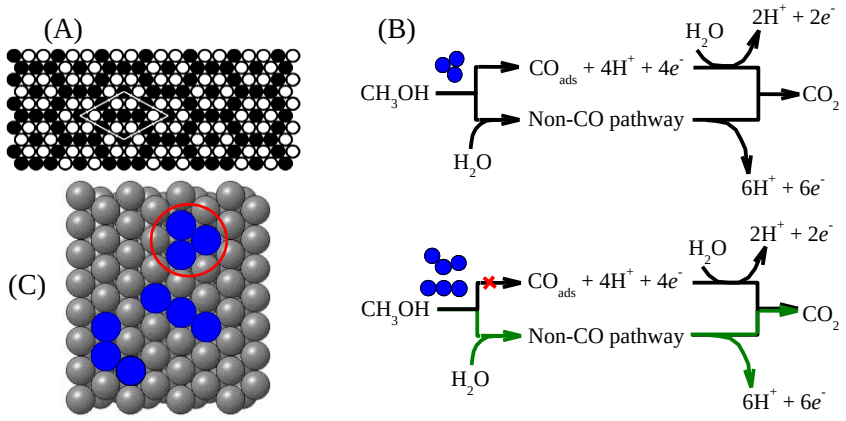

Figure 7. (A): ball model of the $(2\sqrt{3}\times2\sqrt{3})R30^{o}$ structure of the cyanide layer on a Pt(111) surface. (B): possible reaction pathways on specific geometric arrangement of three Pt atoms as (111) terraces. (C): hard sphere model of a Pt(111) surface indicating three possible configuration involving three connected Pt atoms, and the configuration inside the circle being the only one that allows the CO_{ads} formation from the methanol dissociation. The scheme in (A-B) were reproduced and adapted from [70] American Chemical Society with permission.

At least in the case of the cyanide-Pt(111) modified electrode, it was found that at least *three contiguous atoms* at the Pt surfaces are required for the formation of CO_{ads}, while at least two contiguous atoms are required for the activation pathway of CO_2 formation [73]. The set of atoms into the circle in the

Figure 7(C) likely are the "active sites" in the indirect pathway for the methanol electro-oxidation toward CO_2 going through CO_{ads}. In the cyanide-Pt(111) modified electrode, those three contiguous Pt atoms are not available and then the direct pathway takes place. As we can observe in Figure 7(A), the set of three atoms are row of atoms and the condition of the *three contiguous atoms* is not fulfilled on cyanide-Pt(111) modified surfaces. This elegant experiment provide exactly the narrow relationship existent between specific set of atoms on the catalyst and the specific reaction pathways.

Similar restriction of *at least three contiguous Pt atoms* was also observed for formic acid to be electro-oxidized to CO_2 with going through CO_{ads} on cyanide-Pt(111) modified electrodes [74]. In conclusion, the mechanisms of methanol electro-oxidation imply that at least two contiguous atoms of Pt are required for the activation of the reaction pathway of CO_2 formation, and at least *three contiguous atoms* are needed for the dehydrogenation of the methanol molecule toward CO_{ads}.

3.4. Electro-oxidation of Ammonia

In this reaction, we approach one extreme case in which the electrocatalytic reaction takes place at a single kind of active sites. The interest of ammonia electrochemical oxidation is because this toxic gas, or rather, the ammonium sulfate $(NH_4)_2SO_4$, worldwide used as fertilizer, is a contaminant of water. Then, the development of electrochemical sensors and selective catalysts for the degradation of ammonia to a harmless molecule such as the N_2 gas, are a subject of intense research in electrochemistry [75]. Other interest on the ammonia electro-oxidation is because, from the electrochemical energy conversion point of view, ammonia is a potential candidate to be used as fuel in direct "ammonia" fuel cells [76, 77]. In extreme alkaline media, the standard potential for the ammonia oxidation reaction $NH_{3\,(g)} + 3OH^-_{(aq)} \rightleftarrows \frac{1}{2}N_{2\,(g)} + 3H_2O_{\,(l)} + 3e^-$ is $E^0 \simeq -0.770\ V_{SHE}$ (or $\sim 0.055\ V_{RHE}$) [76]. Then, it is interesting to study catalyst materials on which the selective electrochemical oxidation of ammonia toward N_2 gas is kinetically favored.

In terms of reaction mechanism, the accepted mechanism for the electro-chemical oxidation of ammonia in alkaline media was proposed by Gerischer and Mauerer [78] according to them, it occurs through a sequential dehydrogenation of adsorbed ammonia ($NH_{3,\,ads}$) resulting in NH_x species, *i.e.*, $NH_{2,\,ads}$, $NH_{,\,ads}$, and N_{ads}. The main reaction intermediate is the NH_2 species, which dimerizes to adsorbed hydrazine-like $N_2H_{x+y,\,ads}$, which might easily oxidize to N_2. The complete dehydrogenation of ammonia yields the N_{ads} species which is inert for the formation of N_2, but in kinetics it was considered as a catalytic poison [78]. The essence of the Gerischer-Mauerer mechanism has been corroborated [79, 80] by using DEMS (Differential Electrochemical Mass Spectrometry) at Pt in alkaline solution, in which N_2, NO_2 and NO [79] (byproduct of ammonia oxidation) were identified. In relation to the adsorbed species, Matsui *et al*. [81] by *in situ* ATR – IR (Attenuated Total Reflection Infrared) spectroscopy identified bridge bonded NO_{ads} species on the Pt surface in alkaline media as a catalytic poison (a band due to NH_2 wagging mode of N_2H_4 was detected).

Studies employing Pt basal planes, namely, the Pt(111), Pt(110) and Pt(100), in alkaline media, showed that the electrochemical oxidation reaction of ammonia is extremely structure sensitive and takes place almost exclusively on sites with (100) symmetry [82]. In line with this statement, different voltammetric profiles for ammonia electro-oxidation on Pt basal planes, in alkaline solution, are displayed in Figure 8. The highest current density for the ammonia electro-oxidation on Pt(100) plane evidences the

superior activity of this surface over the other basal planes. A local maximum occurs at ~0.55 V_{RHE}, and at ~0.65 V_{RHE} a pair of redox peaks observed. In subsequent studies employing stepped Pt surfaces consisting of (100) terraces separated by monoatomic steps of (111) or (110) symmetry, revealed that the activity depends on the terrace width [83].

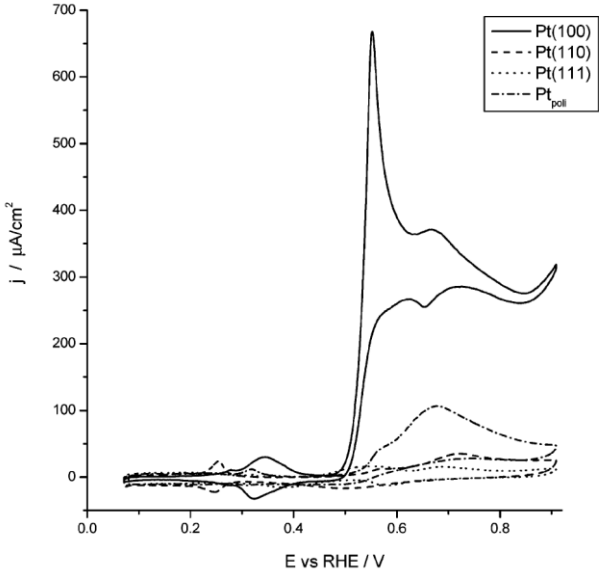

Figure 8. Cyclic voltammetric profiles of the oxidation of 10^{-3} M ammonia on Pt(100), Pt(111) and Pt(110) electrodes and polyoriented Pt single crystal in 0.1 M NaOH. Experiments performed at potential sweep speed of 10 mV s^{-1}. Data were reproduced from [83] American Chemical Society with permission.

However, as pointed out above, different reaction products are formed from ammonia electro-oxidation on platinum [79]. Then, molecular details on the preference of reaction pathways (or selectivity) on Pt single crystals was obtained by DEMS, using a labelled ammonia (^{15}N) in 0.1 M NaOH, and it were detected [84] $^{15}N_2$, ^{15}NO and $^{15}N_2O$, whose mass-charge ration (*m*/*z*) data were reproduced in Figure 9.

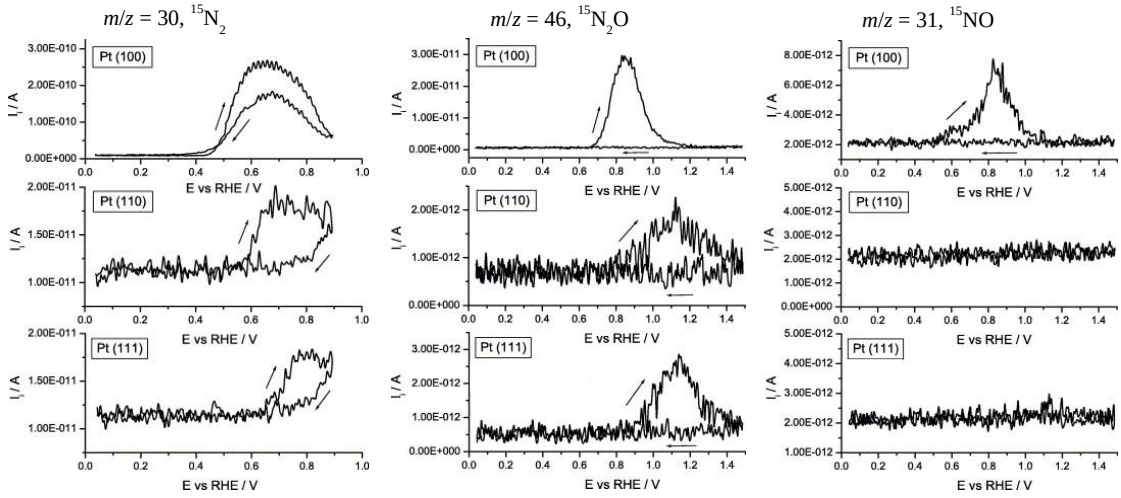

Figure 9. Mass spectrometric cyclic voltammetries curves for the electro-oxidation of 10^{-3} M ammonia ($(^{15}NH_4)_2SO_4$) at three Pt basal surfaces, namely, Pt(100), Pt(111) and Pt(110), in 0.1 M NaOH at scan rate of 10 mV s^{-1}. The mass-charge ration (*m*/*z*) for $^{15}N_2$, $^{15}N_2O$ and ^{15}NO species are indicated in the figure. Data were modified and reproduced from [84] Elsevier with permission.

In Figure 9 (left), the intensity for m/z = 30 ($^{15}N_2$) is about one order of magnitude higher for the Pt(100) plane than the other ones. At Pt(100), if we compare the (order of) magnitudes for m/z = 30 ($^{15}N_2$), m/z = 46 ($^{15}N_2O$) and m/z = 31 (^{15}NO), we conclude that the (100) facets are not only the most active sites, but also they are sites highly selective toward N_2 formation. Almost no current and NO was detected for ammonia electro-oxidation on Pt(110) and Pt(111) surfaces, and only a very small amount (low m/z ration) of NO_2 molecules were formed on those surfaces.

In conclusion, the electro-oxidation of ammonia at Pt surfaces is, at least to the knowledge of this authors, the most sensitive electrocatalytic reaction to the structure of the platinum, so that the electro-oxidation of ammonia has served as a guide for the characterization of shape-controlled Pt nanoparticles with (100) preferential orientation [85]. The electrochemical reduction of nitrite (NO_2^-) toward N_2 is another electrocatalytic reaction that preferentially takes place on the (100) facet of the Pt [86], whose reaction mechanism (in terms of intermediates of reactions) has been claimed has some similarity with oxidation mechanism of NH_3 to N_2 [87]. Returning to the reaction mechanism of ammonia electro-oxidation on Pt(100) in alkaline media, recently, Katsounaros *et al*. [80] proposed that the dimerization of $NH_{,\,ads}$ species to $N_2H_{2,\,ads}$ ones, being the last of which is dehydrogenated to N_2; and the N_{ads} species serves as a reaction intermediate for the formation of byproducts as is the NO_{ads} species. Both N_{ads} and NO_{ads} acting as catalyst poisons.

3.5. Asymmetric Electrocatalysis of the Glucose Oxidation in Intrinsically Chiral Pt Surfaces

As already reported above, the surface of the catalyst might consist in different active sites. The sophistication in heterogeneous catalysis and electrocatalysis upgrades when enantioselective reactions are proposed to the catalyst surface. Comprehensive reviews on the origin of the chiral recognition and the enantioselectivity involving asymmetric catalyst surfaces have been published [88, 89]. Briefly, for fcc (face-centered cubic) metal lattices, the chiral recognition and the possible enantioselectivity are characteristics intrinsically linked to the kink sites. From the surface chemistry point of view, the elegance of the kinked surfaces lies in its intrinsic chiral character, and no matter the width of its terraces, all the kinked surfaces are intrinsically chiral [90]. The chiral surfaces cannot overlap with their mirror image. The kinked surfaces appear at the intercept of the three different basal planes, namely, the (111), (110) and (100), Figure 8. Experimentally, they are obtained by cutting the surface of a stepped surface (intercept of two basal planes) with respect to the third basal plane [91] and the chirality obeys the follow condition $h \neq k \neq l$ and $h \times k \times l \neq 0$, in which the ($hkl$) are the Miller indices [92]. One pair of ideal $(643)^{R\&S}$ chiral faces (enantiomers) of the metals of fcc lattices is displayed in Figure 10. The R (from the Latin *rectus*) and S (from the Latin *sinister*) terminology design the clockwise (111) → (100) → (110) and counter-clockwise (111) ← (100) ← (110) sequence of exposed planes on surface (similar to the Cahn-Ingold-Prelog rules), taking into count the priority of the planes on the basis of its packing density $\rho_{(hkl)}$, *i.e.*, $\rho_{(111)} > \rho_{(100)} > \rho_{(110)}$ [93].

Chiral properties, *i.e*. the chiral recognition and the enantioselectivity on solid catalysts, very often, is introduced by attachment of chiral compounds on non-chiral substrates [89], as the hybrid systems. The disadvantage is that the chiral modifiers may be leached from the solid surfaces, which would deactivate

the chiral properties. The enantioselective recognition has also been obtained by generation of cavities in mesoporous Pt, by electrochemical reduction of Pt ions in presence of a "self-assembled liquid crystal" phase and chiral template molecules [94, 95]. Inherently, the electro-deposited material seems to retain chiral character after removal of the template molecules [94, 95]. However, in view of its well-defined surface structure, for understanding underlying factors controlling the chiral properties, the chiral surfaces must be designed, and in this case, the intrinsically chiral single crystal kinked surface is a suitable template for electrocatalytic studies.

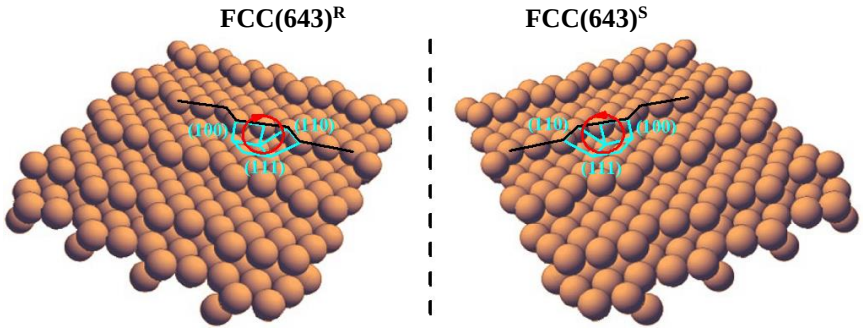

Figure 10. Hard sphere model of a pair of $(643)^{R\&S}$ enantiomer surfaces of metals of fcc lattices. The enantiomer on the right side does not overlap with the surface on the left side. Figure reproduced and adapted from [96] Springer Nature with permission.

As highlighted above, the enantiodifferentiation with kinked surfaces is due to the kink sites; consequently, they are in the origin of the difference in electro-catalytic activity and discrimination of possible reaction pathway at this kind of surface. The first experimental example of enantiospecific interaction/adsorption of chirality on single crystal electrodes was provided in 1999 [97] for the electro-oxidation of D- and L-glucose at the $Pt(643)^R$ and its enantiomorph $Pt(643)^S$ surfaces, respectively, whose surfaces are shown in Figure 10 and the experiments shown in Figure 11 [90]. These kinked surfaces consists in 3 atom width (111) terraces, separated by (110) monoatomic steps broken by sites (100) symmetry, either R or S kink sites – see Figure 10. Firstly, the voltammetry of the $Pt(643)^{S\&R}$ catalysts in presence of the electrolyte (H_2SO_4 or $HClO_4$ solution), present a pair of reversible peaks at ~0.07 and ~0.23 V due to the hydrogen adsorption/desorption at Pt sites [98]. These peaks were shifted toward less positive values in comparison to the Figure 2, because the Pd reference electrode used. The survival of the peak at ~0.07 V suggests that the interaction of the glucose with (110) steps is weak or negligible at low potentials [97, 98], or at low potentials the interaction of either D- or L-glucose is not influenced by the handedness of the Pt(643) surfaces. The important difference in the voltammograms of the enantiomorph $Pt(643)^{S\&R}$ surfaces in presence of D/L-glucose arose for potentials upper to ~0.2 V. Then, in the case of the enantiomorph $Pt(643)^R$ surface, a prominent oxidation peak at ~0.31 V arises for the electro-oxidation of D-glucose Figure 11(b), and this referred peak is absent in electro-oxidation of D-glucose on the enantiomorph $Pt(643)^S$ surface Figure 11(a). For the electro-oxidation of L-glucose, the opposite is observed in Figure 11(c-d): cross-reactivity appears. These examples evidence that the interaction/adsorption of an enantiomer molecules as is the D- or L-glucose (whose molecule structure possess multiple stereochemical center) deeply depends on the chirality of the catalyst surfaces either $Pt(643)^R$ or $Pt(643)^S$.

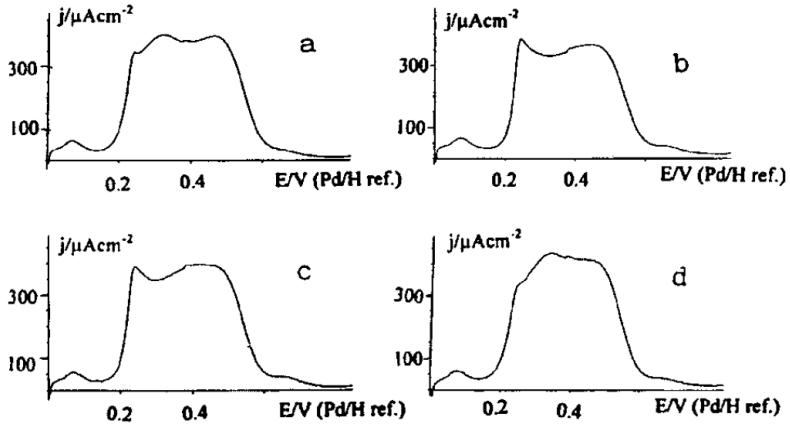

Figure 11. Linear sweep voltammograms of 5×10^{-3} M D-glucose electro-oxidation on: (a) $Pt(643)^S$; (b) $Pt(643)^R$. Linear sweep voltammograms of 5×10^{-3} M L-glucose electro-oxidation on: (c) $Pt(643)^S$; (d) $Pt(643)^R$. Data carried out in 0.1 M H_2SO_4 at potential sweep speed of 50 mV s^{-1} sweep rate. Data reproduced from [90] American Chemical Society with permission.

Clearly, the origin of the enantiodifferentiation on the surfaces is due to the kink sites, likely because of the enantiomer molecule fit better at one kinked surface than in its specular image. The electro-oxidation of L- and D-glucose is very similar on Pt(221) and Pt(332) stepped (non-kinked) surfaces (no chiral recognition).[97] In fact, the increase in the ability in chiral recognition or enantioselectivity excess, apparently coincides with the increase in surface density of kink sites on going from Pt(643) to Pt(321) to Pt(531) surfaces [90]. Because the manifestation of enantioselective character on kinked surfaces requires the presence of kink sites suggests that kinks are the key part of the active sites. Therefore, the kinks in kinked surfaces likely impose the constraint for the interaction between the catalyst and the corresponding reactive stereoisomers. With this regard, at the solid/gas interface, kinetic studies of the desorption of alcohol enantiomers [(*R*)- and (*S*)-2-butanol] from the enantiomorph $Ag(643)^R$ and $Ag(643)^S$ surfaces reported no measurable enantiospecific energy differences of desorption heat, *i.e.*, only ~0.4184 kJ mol^{-1} [99], for those two alcohol enantiomers. In the case of liquid/aqueous electrified interface [90] the difference in reactivity for two (alcohol) isomers is appreciable, which means that energy interactions difference might also be appreciable.

It is worthy to say that the origin of the enantioselective character in kinded surfaces under electrochemical conditions is still much more complex. For example, the chiral recognition seems to depend on the nature of the anion in the electrolyte, being, unexpectedly, the enantioselective difference more marked in presence of strong adsorbing anions (as is the sulfate) than the non-adsorbing anions (as is the case of the perchlorate anion) [98]. Intuitively, the expected results would be of loss in ability of chiral recognition in presence of strong adsorbing anions because this species could block the "active sites" [100], but it is known that anions, as is the (bi)sulfate anions, adsorb at higher potentials at the (111) terrace sites [101]. This fact can explain why there is no inhibition of the hydrogen region in the voltammogram of the $Pt(643)^{R\&S}$ surfaces in presence of glucose in sulfuric acid (Figure 11). Moreover, the kink stability is an incognita because surface reconstruction would modify the surface irreversibly. Indeed, glucose oxidation is a too complex problem to facilitate the understanding of enantiomeric reactivity [102] and clearly more

work is needed to disentangle this problem using pure enough isomers (the key step) with low molecular weight.

4. Concluding Remarks and Prospects

This report illustrates some examples aiming the determination of specific active sites in electrocatalytic reactions which preferentially take place on specific facets of a catalyst consisting of non-equivalent sites. The determination of the active sites for the CO electro-oxidation requires a precise specification of the experimental conditions employed, especially because the catalytic activity of the Pt toward CO electro-oxidation deeply depends on the history of the CO adlayer. Then, for the cases in which a CO adlayer is deposited under potential control, *i.e.*, in the hydrogen region, the main characteristic of the electro-oxidation of CO on Pt catalyst is that the reaction preferentially takes place at the (111) plane of defected surfaces. The preferred reaction on (111) terraces of the defected surfaces combines the action of steps in modifying the catalytic properties at (111) terraces, and the most active sites (that are locally concave structures) and the lowest active ones (that are locally convex structures) are facets of a same local structure at the Pt surfaces. The CO_{ads} is a reaction intermediate formed during the oxidation of methanol. The set of atoms able to activate the direct reaction pathway of methanol electro-oxidation toward CO_2 involve three contiguous atoms. Both surface defects and (111) terraces (111) can provide this set of contiguous atoms. The determination of the active sites for a more complex reaction, such as glucose oxidation, cannot be determined with apparent simplicity like that in the case of CO electro-oxidation. However, it is possible to note that the introduction of the kinks sites is responsible for the appearance of chiral recognition of glucose in kinked surfaces. On the other hand, the determination of the active sites in ammonia oxidation (and also other nitrogen containing species, as nitrite reduction) is easily characterized as being (100) square symmetry, because the extreme difference of electrochemical reactivity among the different sites. Moreover, at this type of sites, the reaction is entirely selective to the N_2 formation, which is the desired product.

This paper is only a step towards determining of the active site on the surfaces of the catalysts in the macroscopic scale. It is mainly centered around Pt(111) and its vicinal surfaces. In this sense, there is a lot of work still necessary on single crystal vicinal to the other two basal planes to make breakthroughs in the identification of active sites and progress forward to incorporate more complex situations, *e.g*. those involving shape-controlled nanoparticles. The macroscopic crystals at some level mimic the surfaces of the shape-controlled nanoparticles, and in this sense, it is interesting to investigate the concepts of stepped surfaces that fit the materials at the nanoscopic scale. Future works should follow these directions.

Acknowledgments

M.J.S.F. is grateful to PNPD/CAPES (Brazil). J.M.F. thanks the MCINN (FEDER) (Spain) project-CTQ-2016-76221-P.

5. References

1 Kirby AJ (1997) Efficiency of proton transfer catalysis in models and enzymes. *Acc Chem Res* 30:290-296.

2 Robert S (2015) Heterogeneous catalysis. *Angew Chem Int Ed* 54:3465-3520.

3 Vojvodic A, Nørskov JK (2015) New design paradigm for heterogeneous catalysts. *Nat Sci Rev* 2:140-143.

4 Andersen M, Medford AJ, Nørskov JK, Reuter K (2017) Scaling-relation-based analysis of bifunctional catalysis: the case for homogeneous bimetallic alloys. *ACS Catal* 7:3960-3967.

5 Norskov JK, Studt F, Abild-Pedersen F, Bligaard T (2014) Fundamental concepts in heterogeneous catalysis. John Wiley & Sons, Inc.

6 Somorjai GA, Li Y (2010) *Introduction to surface chemistry and catalysis*, John Wiley & Sons.

7 Tian N, Zhou ZY, Sun SG, Ding Y, Wang ZL (2007) Synthesis of tetrahexahedral platinum nanocrystals with high-index facets and high electro-oxidation activity. *Science* 316:732-735.

8 Seung WL, Chen S, Sheng W, Yabuuchi N, Kim YT, Mitani T, Vescovo E, Shao-Horn Y (2009) Roles of surface steps on Pt nanoparticles in electro-oxidation of carbon monoxide and methanol. *J Am Chem Soc* 131:15669-15677.

9 Koper MTM (2011) Structure sensitivity and nanoscale effects in electrocatalysis. *Nanoscale* 3:2054-2073.

10 Strmcnik D, Kodama K, van der Vliet D, Greeley J, Stamenkovic VR, Marković NM (2009) The role of non-covalent interactions in electrocatalytic fuel-cell reactions on platinum. *Nat Chem* 1:466.

11 Stoffelsma C, Rodriguez P, Garcia G, Garcia-Araez N, Strmcnik D, Marković NM, Koper MTM (2010) Promotion of the oxidation of carbon monoxide at stepped platinum single-crystal electrodes in alkaline media by lithium and beryllium cations. *J Am Chem Soc* 132:16127-16133.

12 Gale RJ, Salmeron M, Somorjai GA (1977) Variation of surface reaction probability with reactant angle of incidence: a molecular beam study of the asymmetry of stepped platinum crystal surfaces for H-H bond breaking. *Phys Rev Lett* 38:1027-1029.

13 O'Mullane AP (2014) From single crystal surfaces to single atoms: investigating active sites in electrocatalysis. *Nanoscale* 6:4012-4026.

14 Koper M, Wieckowski A (2009) *Fuel Cell Catalysis: A Surface Science Approach*, Wiley.

15 Koper MTM (2005) Combining experiment and theory for understanding electrocatalysis. *J Electroanal Chem* 574:375-386.

16 Seh ZW, Kibsgaard J, Dickens CF, Chorkendorff I, Nørskov JK, Jaramillo TF (2017) Combining theory and experiment in electrocatalysis: Insights into materials design. *Science* 355.

17 Taylor HS (1925) A theory of the catalytic surface. *Proc R Soc London. Series A* 108, 105-111.

18 Buurmans ILC, Weckhuysen BM (2012) Heterogeneities of individual catalyst particles in space and time as monitored by spectroscopy. *Nat Chem* 4:873-886.

19 Wandelt K (1997) The local work function: concept and implications. *App Surf Scie* 111:1-10.

20 Jia JF, Inoue K, Hasegawa Y, Yang WS, Sakurai T (1998) Variation of the local work function at steps on metal surfaces studied with STM. *Phys Rev B* 58:1193-1196.

21 Pérez León C, Drees H, Wippermann SM, Marz M, Hoffmann-Vogel R (2016) Atomic-scale imaging of the surface dipole distribution of stepped surfaces. *J Phys Chem Lett* 7:426-430.

22 Somorjai GA, Park JY (2008) Molecular factors of catalytic selectivity. *Angew Chem Int Ed* 47:9212-9228.

23 Nørskov JK, Bligaard T, Hvolbæk B, Abild-Pedersen F, Chorkendorff I, Christensen CH (2008) The nature of the active site in heterogeneous metal catalysis. *Chem Soc Rev* 37:2163-2171.

24 Batista EA, Malpass GRP, Motheo AJ, Iwasita T (2004) New mechanistic aspects of methanol oxidation. *J Electroanal Chem* 571:273-282.

25 Farias MJS, Mello GAB, Tanaka AA, Feliu JM (2017) Site-specific catalytic activity of model platinum surfaces in different electrolytic environments as monitored by the CO oxidation reaction. *J Catal* 345:216-227.

26 Clavilier J, El Achi K, Rodes A (1990) In situ probing of step and terrace sites on Pt(S)-[n(111) × (111)] electrodes. *Chem Phys* 141:1-14.

27 Rodes A, El Achi K, Zamakhchari MA, Clavilier J (1990) Hydrogen probing of step and terrace sites on Pt(S)-[n(111)×(100)]. *J Electroanal Chem* 284:245-253.

28 Kunimatsu K, Senzaki T, Samjeské G, Tsushima M, Osawa M (2007) Hydrogen adsorption and hydrogen evolution reaction on a polycrystalline Pt electrode studied by surface-enhanced infrared absorption spectroscopy. *Electrochim Acta* 52:5715-5724.

29 Paleček D, Tek G, Lan J, Iannuzzi M, Hamm P (2018) Characterization of the platinum–hydrogen bond by surface-sensitive time-resolved infrared spectroscopy. *J Phys Chem Lett* 9:1254-1259.

30 McCrum IT, Chen X, Schwarz KA, Janik MJ, Koper MTM (2018) Effect of step density and orientation on the apparent pH dependence of hydrogen and hydroxide adsorption on stepped platinum surfaces. *J Phys Chem C* 122:16756-16764.
31 Smoluchowski, R. 1941 Anisotropy of the electronic work function of metals. *Phys Rev* 60:661-674.
32 Climent V, Feliu JM (2011) Thirty years of platinum single crystal electrochemistry. *J Solid State Electrochem* 15:1297-1315.
33 Gómez-Marín AM, Clavilier J, Feliu JM (2013) Sequential Pt(111) oxide formation in perchloric acid: an electrochemical study of surface species inter-conversion. *J Electroanal Chem* 688:360-370.
34 Huang YF, Kooyman PJ, Koper MTM (2016) Intermediate stages of electrochemical oxidation of single-crystalline platinum revealed by in situ Raman spectroscopy. *Nat Commun* 7:12440.
35 Freund HJ, Meijer G, Scheffler M, Schlögl R, Wolf M (2011) CO oxidation as a prototypical reaction for heterogeneous processes. *Angew Chem Int Ed* 50:10064-10094.
36 van Spronsen MA, Frenken JWM, Groot IMN (2017) Surface science under reaction conditions: CO oxidation on Pt and Pd model catalysts. *Chem Soc Rev* 46:4347-4374.
37 Beden B, Lamy C, de Tacconi NR, Arvia AJ (1990) The electrooxidation of CO: a test reaction in electrocatalysis. *Electrochim Acta* 35:691-704.
38 Marković NM, Ross PN (2002) Surface science studies of model fuel cell electrocatalysts. *Surf Sci Rep* 45:117-229.
39 Chen QS, Solla-Gullón J, Sun SG, Feliu JM (2010) The potential of zero total charge of Pt nanoparticles and polycrystalline electrodes with different surface structure: the role of anion adsorption in fundamental electrocatalysis. *Electrochim Acta* 55:7982-7994.
40 Garrick TR, Moylan TE, Carpenter MK, Kongkanand A (2017) Electrochemically active surface area measurement of aged Pt alloy catalysts in PEM fuel cells by CO stripping. *J Electrochem Soc* 164:F55-F59.
41 Moniri S, van Cleve T, Linic S (2017) Pitfalls and best practices in measurements of the electrochemical surface area of platinum-based nanostructured electro-catalysts. *J Catal* 345:1-10.
42 Ye JY, Jiang YX, Sheng T, Sun SG (2016) In-situ FTIR spectroscopic studies of electrocatalytic reactions and processes. *Nano Energy* 29:414-427.
43 Lebedeva NP, Koper MTM, Herrero E, Feliu JM, van Santen RA (2000) Cooxidation on stepped Pt[n(111)×(111)] electrodes. *J Electroanal Chem* 487:37-44.
44 Farias MJS, Cheuquepán W, Tanaka AA, Feliu JM (2018) Requirement of initial long-range substrate structure in unusual CO pre-oxidation on Pt(111) electrodes. *Electrochem Commun* 97:60-63.
45 Gilman S (1964) The mechanism of electrochemical oxidation of carbon monoxide and methanol on platinum. The "Reactant-Pair" mechanism for electrochemical oxidation of carbon monoxide and methanol. *J Phys Chem* 68:70-80.
46 Angelucci CA, Nart FC, Herrero E, Feliu JM (2007) Anion re-adsorption and displacement at platinum single crystal electrodes in CO-containing solutions. *Electrochem Commun* 9:1113-1119.
47 Ueno T, Tanaka H, Sugawara S, Shinohara K, Ohma A, Hoshi N, Nakamura M (2017) Infrared spectroscopy of adsorbed OH on n(111)-(100) and n(111)-(111) series of Pt electrode. *J Electroanal Chem* 800:162-166.
48 Santos E, Leiva EPM, Vielstich W (1991) CO adsorbate on Pt(111) single crystal surfaces. *Electrochim Acta* 36, 555-561.
49 Farias MJS, Busó-Rogero C, Gisber R, Herrero E, Feliu JM (2014) Influence of the CO adsorption environment on its reactivity with (111) terrace sites in stepped Pt electrodes under alkaline media. *J Phys Chem C* 118:1925-1934.
50 García G, Koper MTM (2008) Stripping voltammetry of carbon monoxide oxidation on stepped platinum single-crystal electrodes in alkaline solution. *Phys Chem Chem Phys* 10:3802-3811.
51 Farias MJS, Herrero E, Feliu JM (2013) Site selectivity for CO adsorption and stripping on stepped and kinked platinum surfaces in alkaline medium. *J Phys Chem C* 117:2903-2913.
52 Farias MJS, Camara GA, Feliu JM (2015) Understanding the CO preoxidation and the intrinsic catalytic activity of step sites in stepped Pt surfaces in acidic medium. *J Phys Chem C* 119:20272-20282.
53 Herrero E, Chen QS, Hernandez J, Sun SG, Feliu JM (2011) Effects of the surface mobility on the oxidation of adsorbed CO on platinum electrodes in alkaline media. The role of the adlayer and surface defects. *Phys Chem Chem Phys* 13:16762-16771.

54 Lebedeva NP, Rodes A, Feliu JM, Koper MTM, van Santen RA (2002) Role of crystalline defects in electrocatalysis: CO adsorption and oxidation on stepped platinum electrodes as studied by in situ infrared spectroscopy. *J Phys Chem B* 106:9863-9872.

55 Calle-Vallejo F, Pohl MD, Bandarenka AS (2017) Quantitative coordination - activity relations for the design of enhanced Pt catalysts for CO electro-oxidation. *ACS Catal* 7:4355-4359.

56 Farias MJS, Vidal-Iglesias FJ, Solla-Gullón J, Herrero E, Feliu JM (2014) On the behavior of CO oxidation on shape-controlled Pt nanoparticles in alkaline medium. *J Electroanal Chem* 716:16-22.

57 McPherson IJ, Ash PA, Jones L, Varambhia A, Jacobs RMJ, Vincent KA (2017) Electrochemical CO oxidation at platinum on carbon studied through analysis of anomalous in situ IR spectra. *J Phys Chem C* 121:17176-17187.

58 Backus EHG, Eichler A, Kleyn AW, Bonn M (2005) Real-time observation of molecular motion on a surface. *Scie* 310:1790-1793.

59 Farias MJS, Cheuquepán W, Tanaka AA, Feliu JM (2018) Unraveling the nature of active sites in ethanol electro-oxidation by site-specific marking of a Pt catalyst with isotope-labeled ^{13}CO. *J Phys Chem Lett* 9:1206-1210.

60 Farias MJS, Cheuquepán W, Tanaka AA, Feliu JM (2017) Nonuniform synergistic effect of Sn and Ru in site-specific catalytic activity of Pt at bimetallic surfaces toward CO electro-oxidation. *ACS Catal* 7:3434-3445.

61 Vielstich W (2003) Electrochemical energy conversion: methanol fuel cell as example. *J Brazilian Chem Soc* 14:503-509.

62 Cuesta A (2017) Electrooxidation of C_1 organic molecules on Pt electrodes. *Curr Opinion Electrochem* 4:32-38.

63 Herrero E, Feliu JM (2018) Understanding formic acid oxidation mechanism on platinum single crystal electrodes. *Curr Opinion Electrochem* 9:145-150.

64 Grozovski V, Climent V, Herrero E, Feliu JM (2010) Intrinsic activity and poisoning rate for HCOOH oxidation on platinum stepped surfaces. *Phys Chem Chem Phys* 12:8822-8831.

65 Grozovski V, Climent V, Herrero E, Feliu JM (2011) The role of the surface structure in the oxidation mechanism of methanol. *J Electroanal Chem* 662:43-51.

66 Miki A, Ye S, Osawa M (2002) Surface-enhanced IR absorption on platinum nanoparticles: an application to real-time monitoring of electrocatalytic reactions. *Chem Commun* 1500-1501.

67 Chen YX, Heinen M, Jusys Z, Behm RJ (2006) Bridge-bonded formate: Active intermediate or spectator species in formic acid oxidation on a Pt film electrode? *Langmuir* 22, 10399-10408.

68 Osawa M, Komatsu KI, Samjeské G, Uchida T, Ikeshoji T, Cuesta A, Gutiérrez C (2011) The role of bridge-bonded adsorbed formate in the electrocatalytic oxidation of formic acid on platinum. *Angew Chem Int Ed* 50:1159-1163.

69 Iwasita T (2002) Electrocatalysis of methanol oxidation. *Electrochimica Acta* 47:3663-3674.

70 Cuesta A (2006) At least three contiguous atoms are necessary for CO formation during methanol electrooxidation on platinum. *J Am Chem Soc* 128:13332-13333.

71 Villegas I, Weaver MJ (1994) Carbon monoxide adlayer structures on platinum (111) electrodes: a synergy between in-situ scanning tunneling microscopy and infrared spectroscopy. *J Chem Phys* 101:1648-1660.

72 Kim YG, Yau SL, Itaya K (1996) Direct observation of complexation of alkali cations on cyanide-modified Pt(111) by scanning tunneling microscopy. *J Am Chem Soc* 118:393-400.

73 Angel C (2011) Atomic ensemble effects in electrocatalysis: the site-knockout strategy. *ChemPhysChem* 12:2375-2385.

74 Cuesta A, Escudero M, Lanova B, Baltruschat H (2009) Cyclic voltammetry, FTIRS, and DEMS study of the electrooxidation of carbon monoxide, formic acid, and methanol on cyanide-modified Pt(111) electrodes. *Langmuir* 25:6500-6507.

75 Valentini F, Biagiotti V, Lete C, Palleschi G, Wang J (2007) The electrochemical detection of ammonia in drinking water based on multi-walled carbon nanotube/copper nanoparticle composite paste electrodes. *Sens Actuators B Chem* 128:326-333.

76 Simons EL, Cairns EJ, Surd DJ (1969) The Performance of direct ammonia fuel cells. *J Electrochem Soc* 116:556-561.

77 Acevedo R, Poventud-Estrada CM, Morales-Navas C, Martínez-Rodríguez RA, Ortiz-Quiles E, Vidal-Iglesias FJ, Sollá-Gullón J, Nicolau E, Feliu JM, Echegoyen L, et al (2017) Chronoamperometric study of ammonia oxidation in a direct ammonia alkaline fuel cell under the influence of microgravity. *Microgravity Sci Technol* 29:253-261.

78 Gerischer H, Mauerer A (1970) Untersuchungen zur anodischen oxidation von ammoniak an platin-elektroden. *J Electroanal Chem* 25:421-433.

79 Wasmus S, Vasini EJ, Krausa M, Mishima HT, Vielstich W (1994) DEMS-cyclic voltammetry investigation of the electrochemistry of nitrogen compounds in 0.5 M potassium hydroxide. *Electrochim Acta* 39:23-31.

80 Katsounaros I, Figueiredo MC, Calle-Vallejo F, Li H, Gewirth AA, Markovic NM Koper MTM (2018) On the mechanism of the electrochemical conversion of ammonia to dinitrogen on Pt(1 0 0) in alkaline environment. *J Catalysis* 359:82-91.

81 Matsui T, Suzuki S, Katayama Y, Yamauchi K, Okanishi T, Muroyama H, Eguchi K (2015) In situ attenuated total reflection infrared spectroscopy on electrochemical ammonia oxidation over Pt electrode in alkaline aqueous solutions. *Langmuir* 31:11717-11723.

82 Vidal-Iglesias FJ, García-Aráez N, Montiel V, Feliu JM, Aldaz A (2003) Selective electrocatalysis of ammonia oxidation on Pt(100) sites in alkaline medium. *Electrochem Commun* 5:22-26.

83 Vidal-Iglesias FJ, Solla-Gullón J, Montiel V, Feliu JM, Aldaz A (2005) Ammonia selective oxidation on Pt(100) sites in an alkaline medium. *J Phys Chem B* 109:12914-12919.

84 Vidal-Iglesias FJ, Solla-Gullón J, Feliu JM, Baltruschat H, Aldaz A (2006) DEMS study of ammonia oxidation on platinum basal planes. *J Electroanal Chem* 588:331-338.

85 Martínez-Rodríguez RA, Vidal-Iglesias FJ Solla-Gullón J, Cabrera CR, Feliu JM (2014) Synthesis of Pt nanoparticles in water-in-oil microemulsion: effect of HCl on their surface structure. *J Am Chem Soc* 136:1280-1283.

86 Duca M, Figueiredo MC, Climent V, Rodriguez P, Feliu JM, Koper MTM (2011) Selective catalytic reduction at quasi-perfect Pt(100) domains: a universal low-temperature pathway from nitrite to N_2. *J Am Chem Soc* 133:10928-10939.

87 Finkelstein DA, Bertin E, Garbarino S, Guay D (2015) Mechanistic similarity in catalytic N_2 production from NH_3 and NO_2 – at Pt(100) thin films: toward a universal catalytic pathway for simple N-containing species, and its application to in situ removal of NH_3 poisons. *J Phys Chem C* 119:9860-9878.

88 Mallat T, Orglmeister E, Baiker A (2007) Asymmetric catalysis at chiral metal surfaces. *Chem Rev* 107:4863-4890.

89 Zaera F (2017) Chirality in adsorption on solid surfaces. *Chem Soc Rev* 46:7374-7398.

90 Attard GA (2001) Electrochemical studies of enantioselectivity at chiral metal surfaces. *J Phys Chem B* 105:3158-3167.

91 Climent V, Feliu JM (2017) Surface electrochemistry with Pt single-crystal electrodes. In *Advances in Electrochemical Science and Engineering*, pp.1-57, Wiley-VCH Verlag GmbH & Co. KGaA.

92 Sholl DS, Asthagiri A, Power TD (2001) Naturally chiral metal surfaces as enantiospecific adsorbents. *J Phys Chem B* 105:4771-4782.

93 Attard GA, Clavilier J, Feliu JM (2002) Chirality at well-defined metal surfaces. In *Chirality: Physical Chemistry*. pp.254-268, American Chemical Society.

94 Wattanakit C, Côme YBS, Lapeyre V, Bopp PA, Heim M, Yadnum S, Nokbin S, Warakulwit C, Limtrakul J, Kuhn A (2014) Enantioselective recognition at mesoporous chiral metal surfaces. *Nat Commun* 5:3325.

95 Yutthalekha T, Wattanakit C, Lapeyre V, Nokbin S, Warakulwit C, Limtrakul J, Kuhn A (2016) Asymmetric synthesis using chiral-encoded metal. *Nat Commun* 7:12678.

96 Gellman AJ, Ernst KH (2018) Chiral autocatalysis and mirror symmetry breaking. *Catal Lett* 148:1610-1621.

97 Ahmadi A, Attard G, Feliu J, Rodes A (1999) Surface reactivity at “chiral” platinum surfaces. *Langmuir* 15:2420-2424.

98 Attard GA, Harris C, Herrero E, Feliu J (2002) The influence of anions and kink structure on the enantioselective electro-oxidation of glucose. *Faraday Discussions* 121:253-266.

99 McFadden CF, Cremer PS, Gellman AJ (1996) Adsorption of chiral alcohols on “chiral” metal surfaces. *Langmuir* 12:2483-2487.

100 (2002) General Discussion. *Faraday Discussions* 121:331-364.

101 Mostany J, Herrero E, Feliu JM, Lipkowski J (2002) Thermodynamic studies of anion adsorption at stepped platinum(hkl) electrode surfaces in sulfuric acid solutions. *J Phys Chem B* 106:12787-12796.

102 Popović KĐ, Tripković AV, Adžić RR (1992) Oxidation of d-glucose on single-crystal platinum electrodes: a mechanistic study. *J Electroanal Chem* 339:227-245.